ELSEVIER

Chemical Engineering Journal 136 (2008) 66–76

Chemical Engineering Journal

www.elsevier.com/locate/cej

Investigation of H_2 staging effects on CO conversion and product distribution for Fischer–Tropsch synthesis in a structured microchannel reactor

L. Guillou *, S. Paul, V. Le Courtois

Unité de Catalyse et de Chimie du Solide, UMR CNRS 8181, Ecole Centrale de Lille, Cité Scientifique BP-48, 59651 Villeneuve d'Ascq Cedex, France

Received 4 December 2006; received in revised form 16 March 2007; accepted 19 March 2007

Abstract

The effect of H_2 staging for Fischer–Tropsch synthesis over a 20 wt% Co/SiO_2 catalyst in a 200 μL wall-coated channel microreactor was investigated.

Some pre-experimental modeling was developed from a modified pseudo-homogeneous 1D reactor model using a pre-established rate form for CO consumption. The predicted CO conversion levels attained for various discrete staging policies were investigated and the results were used as a pre-selection tool. It was used to design a H_2 staged reactor with three equally spaced injection ports.

The experimental set-up was used to get conversion and product distribution data for various H_2 distribution policies. The experimental conversions were in good agreement with the modeling. The tuning of H_2 flow pattern over the three ports lowered the CO conversion and increased mainly C_5–C_9 selectivity. Once combined, these effects allowed to half the C_1–C_4 yield without dramatically reducing the overall C_{5+} yield allowing a smarter use of H_2. A non-uniform increasing staging policy gave the best product distribution for C_{5+} increased production at 0.1 MPa and 180 °C.

Keywords: Fischer–Tropsch synthesis; Micro-structured reactor; Cross-flow reactor; Conversion simulation; Co catalyst

1. Introduction

The most common feed configuration for fixed-bed reactors may be defined as a co-feed strategy: reactants are mixed and injected in the same inlet. But other feed geometries may be encountered. These are defined as distributed feed as long as multiple inlets are concerned. Reactors using such distribution patterns are generally referred to as cross-flow, staged or distributed/distribution reactors [1]. These generic names may in fact cover various flow configurations and distribution devices. Lu et al. [1–3] proposed six different classes (Fig. 1) depending on either the auxiliary inlets are continuously (Fig. 1(2 and 4)) or discretely (Fig. 1(1, 3, 5 and 6)) distributed, uniformly fed (Fig. 1(2 and 3)) or not (Fig. 1(4–6)) and, in the case of a discrete staging, equally spaced (Fig. 1(3 and 5)) or not (Fig. 1(6)). The choice of a configuration versus another should rely on the properties of the reactions involved such as reaction rates, heat released as well as reaction schemes, etc. According to each situation described by these intrinsic properties, to tune the local reactant partial pressures through a staged injection of one of the reactive streams may be an engineering solution to induce yield or selectivity modifications for a selected product or to avoid undesirable side reaction [4–8].

Fischer–Tropsch synthesis (FT) allows to convert syngas into a broad range of hydrocarbons but it exhibits a relatively complex behaviour. An extensive review of its properties was proposed in a recent tome [9]. FT shows a still unclear and only partially understood reaction scheme, which results on the production of a broad range of hydrocarbon products, plus water and CO_2, the relative quantities of which depending on many reaction parameters such as pressure, temperature or catalyst used [10]. As a consequence it is difficult to define selectivity issues, product distribution being possibly a far proper term. Generally a desired hydrocarbon fraction is aimed at in order to get an economically attractive production, depending on feedstock nature and on process conditions. Within the possible productions, short isoparaffins or unbranched middle distillates appear as two

* Corresponding author. Present address: L.G.P.C., UMR CNRS No. 2214, ESCPE, 43 Boulevard du 11/11/1918, F-69100 Villeurbanne, France.
E-mail address: lgu@lgpc.cpe.fr (L. Guillou).

1385-8947/$ – see front matter © 2007 Elsevier B.V. All rights reserved.
doi:10.1016/j.cej.2007.03.030

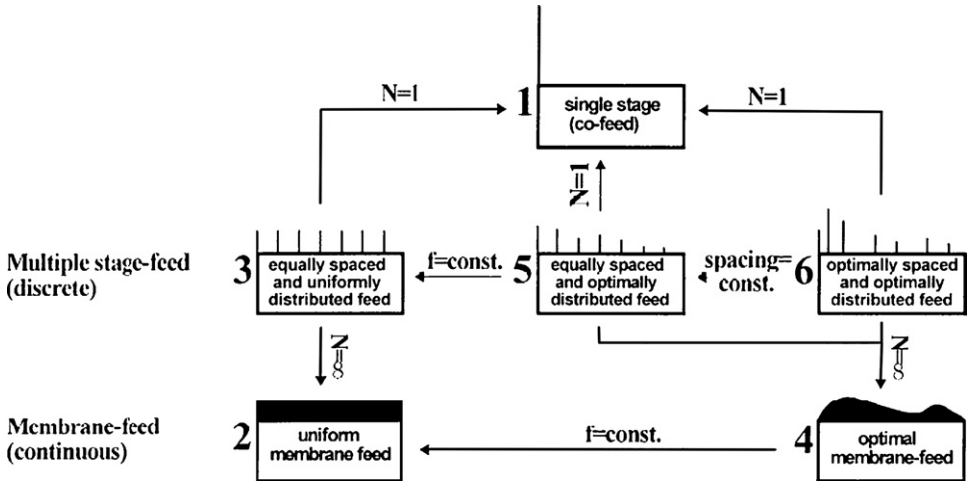

Fig. 1. Six types of feed policies and their interrelations. (The numbers labeled next to the rectangles refer to the types of reactors; N being the number of feed points and f the feed distribution function.) Reprinted from ref. [1], Copyright (1997), with permission from Elsevier.

attractive synfuels. The former may be used as a quality gasoline [11], whereas the properties of the latter make it a hydrocarbon mixture of choice for the blending of diesel fuels for example [12]. For diesel fuel production a catalyst of choice is Co based. It can be assessed from available rate expressions for CO consumption that H_2 distribution would hinder CO conversion [13] but effects on product distribution are less easily predicted. In order to reach their optimal efficiency, Co based catalysts require a P_{H_2}/P_{CO} value set around 2–2.1 [40]. If such a value can be obtained for syngas processed from natural gas, it is not necessary the case for other raw material resources such as coal or biomass: they lead to CO rich syngas feds. In order to be used with Co based catalysts, syngas composition need to be corrected [15]. Question might be addressed on the best way to ensure this correction: either totally upstream of the reactor or through a local dosing of extra H_2 with staging policies. Influence on staging over overall activity and C_{5+} cut selectivity will define a selection criteria defining the potential of H_2 staging.

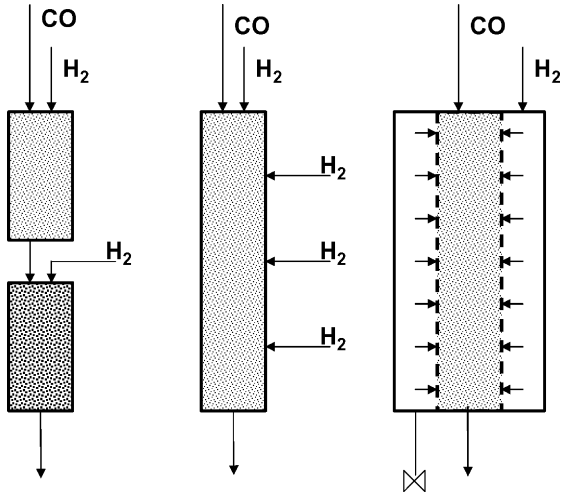

Fig. 2. Schematic view of reported staged reactors for FT (from left to right [13], [14], [9]).

Yet as far as FT is concerned, only a few distributed strategies were experimented [11,16–21] (Fig. 2). A first staged approach was proposed under the form of follow-bed (Fig. 2, left), or two stages, process for the production of isoparaffins by Zhao et al. [11]. The first stage of the process used a typical FT catalyst operated under classical co-feed conditions. The second stage used a HZMS-5 zeolite to crack and isomerize the FT products. An additional H_2 feed between the two stages is required to properly operate the cracking operation. Although using an inter-stage auxiliary hydrogen feed, that process is hardly related to a pure cross-flow system because of the different nature of the two consecutive catalyst beds. A second concept of staging policy for FT processes was proposed [16]: two or more reactors are integrated in a cascading configuration, which includes additional inter-stage gas feeds and optional inter-stage water extractors. If reactors are packed bed, then the process flow sheet tend toward a follow bed configuration as proposed by Zhao et al. [11] at labscale and is somehow close to a distributed reactor. Another feed distribution policy was proposed by Sharifnia et al. [17] with a 4 points discrete feed (Fig. 2, centre). Continuous (membrane) distributors were studied in our group too [18–21] (Fig. 2, right). These membrane set-ups differed from their traditional use in FT as potential devices for water continuous extraction [22–23] or as plug-through contactors [24–26]. The various distributor configurations reported were proposed to get an increased selectivity into C_{5+} or C_{10}–C_{20} syncrude. The configurations considered in these studies used distributors located along a packed-bed. The results obtained by Sharifnia et al. [17] on 2 g of a 22 wt% Co/SiO_2 packed catalyst exhibited an enhancement of C_{5+} selectivity and a decrease of the CH_4 production for various distribution policies at 0.1 MPa and for temperatures and resident times varied between 200 and 220 °C and 1–4 s respectively. The olefinic ratio of the products increased too. These product distribution modifications versus a co-feed strategy were however counter-balanced by a decrease of the CO conversion by a factor of 1.6–2 in regard of the H_2 distribution profile between the four inlets. Globally, C_{5+} yield was only slightly affected under the three tested geometries.

Our group own researches with H_2 membrane distributors and 20 wt% Co/Al_2O_3 [18,20] catalysts showed similar trends for C_1 and C_{5+} selectivity and CO conversion. Over 20 wt% Co/SiO_2, different behaviour was obtained; as previously, C_1 selectivity was reduced as well as CO conversion but C_{5+} selectivity was lowered too [21]. This Co/SiO_2 catalyst was found to show poor reproducibility and might worth being discarded.

Léonard [18] proposed a simple reactor modelling based on a 1D pseudo-homogeneous approach but only apparent kinetic data collected over a limited experimental range was available. It gave good product distribution predictions for C_7–C_{16} range under differential mode but computed results had a limited interest as they did not succeeded in giving a reliable simulation of the entire product range (the light gases production was largely underestimated) and were restricted to low conversion levels (i.e. CO conversion levels no larger than 8%).

The objective of this work is to contribute to the understanding of the effects of the staging of the H_2 feed on the FT products distribution by combining modelling and a complementary experimental approach. On purpose, a channel micro-reactor with catalyst coated oppositely to the injectors was used to overcome the previously identified drawbacks of the packed-bed systems, mainly in terms of transfer rates: the coated microchannel design is indeed known to be favourable to a more easily achieved isothermal operation and a fast mixing [27] between the added H_2 feeds and the main stream. Although promising and largely investigated in fine chemicals, the use of microstructured reactors for FT remains a rather confidential application field. It appears that only a few papers or patents [28–33] are dedicated to it and most are contributions of Pacific Northwest National Lab [29,30] or spun-off Velocys Corp. teams [31–33]. They focus upon packed or coated channels or arrays but never seemed to address, in the open scientific literature, any feed policy effect beside standard co-feed studies.

In this paper, the influence of various H_2 staging strategies on CO conversion rate was first studied by a modelling approach. The simulation used a simple pseudo-homogeneous 1D model coping with the spatial disposition of the injectors through a distribution function. This exploratory study defined a pre-experimental development stage, which was used as a design tool to select a peculiar staged reactor configuration for complementary experimental study. Experimental results were then considered in order to check out the validity of computed CO conversion trends and to complete them with product distribution and hydrocarbon yield information, not accessible by the simplified modelling method used.

2. Exploratory modeling of H_2 staging effect on X_{CO}

2.1. Model parameters

Most contacting patterns may be simulated providing a rate form for CO consumption is available and well defined over the operational window considered. A power law rate form was previously established for the 20 wt% Co/SiO_2 catalyst used for this contribution [34]. Its parameters were fitted from X_{CO} experimental results obtained for low temperature (150–220 °C) and low pressure FT processes under medium conversion regimes (up 25%). These experiments were achieved in a 200 μL microchamber reactor operated over the 3.6–63.2 mg, 1.5–3 $P^0_{H_2}/P^0_{CO}$ and 0.5–2 s catalyst mass, partial pressure ratio and gas hour spatial velocity ranges, respectively. Total pressure was set constant at 0.1 MPa and 83 mL/h N_2 STP was mixed with the reactants. A best parameter fit gave a power law form

$$-r_{CO} = 0.011 \times P_{CO}^{-0.5} \times P_{H_2}^{0.75} \text{ at } 180\,^{\circ}\text{C (in mol}_{CO}\,\text{s}^{-1}\,\text{atm}^{-0.25}\,\text{kg}_{cat}^{-1})$$

Corresponding activation energy was estimated at 79 (±4) kJ mol^{-1}. Fitted parameters were within the range of published values for power-law rate forms for CO consumption over various Co based catalysts [35–36]. The validity range of this power law was established up to $X_{CO} = 25\%$ at steady state.

This power law rate equation was used in conjunction with a reactor model, which was derived from an isothermal 1D pseudo-homogeneous model. Co-feeding and various distribution strategies were considered in order to simulate conditions relevant of various patterns as defined by Lu et al. [1]. The pre-experimental simulation focused upon continuous and multiple equally spaced discrete distributors. H_2 molar flow added to fit to the selected staging policy was implemented thanks to different distribution functions [1]. The discrete equally spaced and uniformly distributed auxiliary feeds were additionally considered for 3, 4, 6 and 15 ports along a 800 mm long channel. Strategies used for the three equally spaced ports with non-uniform staged feed flow rates followed distribution templates described in Table 1.

Extra-hypotheses were required to cope with partial pressure variations linked to the various product formation rates under integral reactor. A first one was used to define the molar flow variation induced by the water (w) and hydrocarbon (HC) formation. It was defined from a constant molar contraction factor (ε_a). ε_a was defined as the ratio of the number of mole produced in respect of the reactant required for its irreversible production. It must be emphasised that ε_a can be defined only for FT operated under dry mode, i.e. with negligible liquid product formation at reactor pressure and temperature [34]. These conditions are generally acceptable for reaction at atmospheric pressure and low temperature. Moreover, in the present case, the use of ε_a requires to consider that only paraffinic products are formed which restraints its use to catalysts with higher hydrogenation activity, such as cobalt based ones for example. ε_a is expressed for each product with i carbons using a generic product formation equation defined as:

$$iCO + (2i+1)H_2 \rightarrow C_iH_{2i+2} + iH_2O$$

$$\text{and :} \quad \varepsilon_{ai} = \frac{n_{ai}^{out}}{n_{ai}^{in}} = \frac{i+1}{3i+1}$$

where n_{ai} represents the total number of gaseous species either at inlet or outlet for the formation of hydrocarbon with i carbons. ε_{ai} can therefore take any value between 1/3 and 1/2, which are respectively representing the formations of a single infinitely long paraffin or methane exclusively. It must be pondered

Table 1
Non-uniform and uniform feed policies for three ports staged H_2 distributor

	Strategy					
	Co-feed	Staged (≫)	Staged (>)	Staged (=)	Staged (<)	Staged (≪)
H_2 distribution						
Main (a)	100%	66%	44%	33%	22%	11%
Port 1 (b)	0%	22%	33%	33%	33%	22%
Port 2 (c)	0%	11%	22%	33%	44%	66%

using the global extend of reaction through the calculation of an effective ε_{ai}:

$$\varepsilon_{ai}^{\text{eff}} = \varepsilon_{ai} \times x_i$$

with x_i the molar fraction of product i taken from:

$$x_i = \frac{r_{C_iH_{2i+2}}}{\sum r_{C_iH_{2i+2}}}$$

For complex mixture, final ε_a value would be defined as the sum of all the contributions of i^{th} order:

$$\varepsilon_a = \sum \varepsilon_{ai}^{\text{eff}}$$

However, in absence of any model for product distribution prediction and the individual values of $r_{C_iH_{2i+2}}$, it was arbitrary considered that ε_a could be represented by a constant value (i.e. it was assumed that ε_a was product distribution independent) and set at the mean value of 0.417. It was used to calculate an approximate w + HC molar flow through:

$$F_{\text{w+HC}}^{i+1} = F_{\text{w+HC}}^{i} + \varepsilon_a \times (\Delta F_{CO} + \Delta F_{H_2})$$

The variation of F_{CO} and F_{H_2} associated to the reaction is calculated at each integration step. It is used to get the total molar flow variation in respect of the z coordinate which is a function of both $-r_{CO}$ (or X_{CO}) and ε_a.

A second hypothesis was a constant value of the total injected reactants mass flows. Thus the integral value of $n_{H_2}^t/n_{CO}^t$ ratio over the whole longitudinal (z) coordinate was set at a constant value of 2. It can be set under equation as:

$$\frac{n_{H_2}^t}{n_{CO}^t} = \frac{\int_0^z n_{H_2}^0(z)\,dz}{n_{CO}^0} = 2$$

Finally it will be assumed that $-r_{CO} = -r_{CO+H_2}$ [35].

Simulations were done considering a reactor operated at $P = 0.1$ MPa and $T = 180\,^{\circ}C$. The flow values used for the modelling were set at 200 and 60 mL h^{-1} for CO and N_2, respectively. They were considered as being well mixed at inlet. Total H_2 flow used in the modelling was set constant at 400 mL h^{-1} whatever the distribution function considered. Integration argument varied from $z = 0$ to 800 mm. Total exposed catalytic mass over the 800 mm long channel was considered to be 70 mg. Thus required catalyst mass in each cell of the model was 0.0875 mg.

2.2. Influence of the number of ports for equally distributed H_2 flows

The first set of simulations explored the influence of the number of ports. These were equally spaced along the channel and uniformly fed with H_2. Three, 4, 6, 15 inlets were used for discrete distribution. A continuous case (continuous distribution) was studied too.

The number of equally distributed auxiliary inlets showed an influence on the achieved conversion level (Table 2). The simulations predicted a progressive lowering of CO conversion with the increasing number of stages, in reason of a lower activity level computed for sections fed under low H_2/CO conditions. For example, in three-port configuration, first section is under $H_2/CO = 0.66$ at inlet and reached only circa 2 at third inlet, minus H_2 and CO consumed up-flow. This diminution of X_{CO} versus the co-feed strategy was more extensive for policies using a limited number of stages: beyond 10 ports, the conversion loss induced by any additional inlet became negligible, X_{CO} progressively tending toward the asymptotic value of 11.86% reached for a uniformly continuous distributor (membrane like) (Fig. 3). The most impressive loss was thus obtained for the switch from co-feed to three inlets. It actually cost more than 23% of X_{CO} maximum conversion achieved under co-feed policy. Further addition of supplementary inlets showed less influence, the maximum expected conversion tending readily toward the asymptotic value predicted for continuous distribution.

The switch from co-fed to distributed feed policy might therefore be relevant of a progressive shift of the performances as far as conversion is concerned. The number of port may be used to define this behavioural mutation and a number set at three iso-distributed inlets appears as an arbitrary bound-

Table 2
Simulated X_{CO} values for uniformly staged H_2 feed for various numbers of equally spaced ports and for uniformly and non-uniformly staged H_2 feed over three equally spaced ports

	X_{CO} (%)
Number of port	
Co-feed (1)	19.62
3	15.06
4	14.42
6	13.65
15	12.60
Continuous (∞)	11.86
Staging policy	
Co-feed	19.62
≫	17.83
>	16.25
=	15.06
<	13.68
≪	11.34

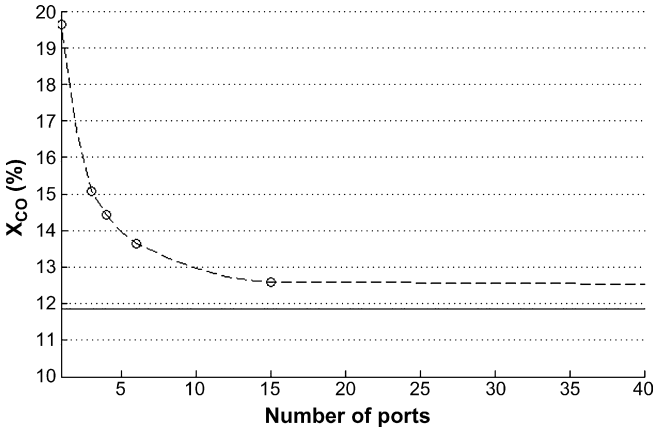

Fig. 3. Simulated variation of X_{CO} in function of the number of reactor stages for a uniform distribution.

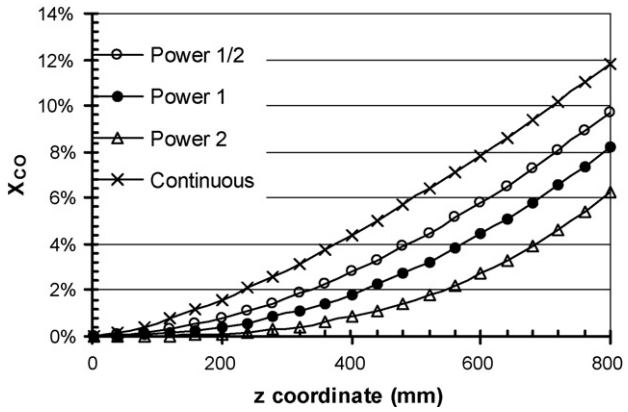

Fig. 5. Simulated cumulated X_{CO} over a single 800 mm long channel for a uniform and three different continuous non-uniform H_2 staging policies.

ary worth being investigated. It may allow to checkout the experimentally achievable conversion levels and the associated product distribution with a reasonable amount of different staging policies from decreasing to increasing staged injection strategies. Additionally, a three-port design can operationally be achieved in a limited time extend for a limited associated cost in microstructured stacked reactors [34]: individual process control and regulation at each inlet remains possible and very little supplementary mechanical or material engineering is required versus a basic microchannel reactor.

2.3. Influence of flow uniformity

Influence of flow uniformity was investigated over continuous and 3 points discrete H_2 distribution. For continuous distributors the added H_2 flow was considered as being uniform or non-uniform. The latter was declined under three possible distributions patterns which were defined using square root, first or second order distribution functions (Fig. 4). The influence of staging uniformity over X_{CO} for the three discrete and equally spaced ports was investigated according to the template defined in Table 1.

For continuous distributors, the simulated conversion levels were highly dependant on the staging uniformity (Fig. 5). For three distribution patterns applied, the order of the function used to define the local additional H_2 injection dramatically modified the achieved conversion: the higher the order, the lower the conversion. For a uniform distribution (order 0) 11.86% of conversion was obtained (Table 2). This level dropped to circa 8.4 and 6.4% for first and second order forms respectively (Fig. 5). For power 2-form distribution function the total conversion loss in respect of the co-feed strategy was reaching 68% versus "only" 40% for a uniformly distributed H_2.

For discrete equally spaced three-port injection policies, the non-uniformity of the feed had similar effect (Table 2). Once again, the later the H_2 was added, the bigger the loss was. For configuration $\ll$, where a maximum of H_2 shortcuts the first two-thirds of the channel, 42.2% of CO conversion were lost. X_{CO} shift toward lower overall activity levels was more progressive over the first policies $\gg$, $>$ and uniform ($=$) which guaranteed a lower H_2 depletion level at reactor main inlet. An insight of X_{CO} as a function of reactor coordinate (Fig. 6) indicated that it was mainly the first part of the reaction zone that presented the most impressive conversion modification under staging strategy.

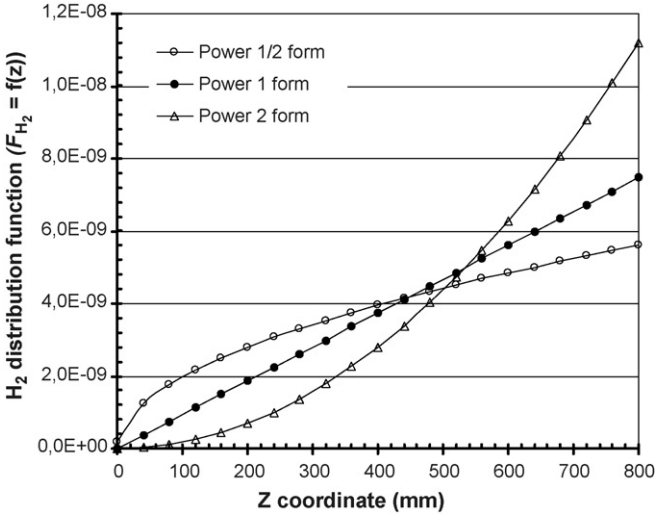

Fig. 4. Distributed H_2 molar flows for three continuous non-uniform staging policies.

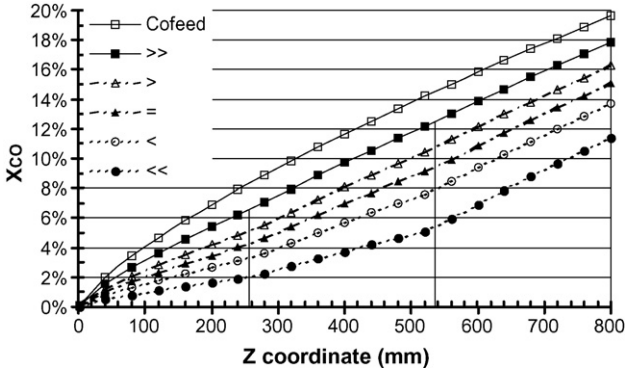

Fig. 6. Simulated cumulated X_{CO} over a single 800 mm long channel for co-feed, uniformly and no-uniformly discrete H_2 staging policies over three equally spaced ports; port locations indicatively shown.

Beyond the first auxiliary port, the conversion profiles tend to become parallel; the most delayed H_2 injections did not appear as causing any outburst of CO conversion for the imposed total H_2 molar flow.

Although simplified, these X_{CO} modelling finally appear as being reasonable under the current retained hypothesis and state of understanding of FT activity over Co catalyst [10,37]: low local P_{H_2}/P_{CO} values tend to decrease the conversion level. The various distribution functions and number of ports considered together or separately just act as different cantilevers to tune this P_{H_2}/P_{CO} local value. Anyway in absence of a potential convenient model for FT product formation at low temperature and pressure, only a complementary experimental campaign can give an insight of staging policies influence over product distribution.

3. Experimental

From the previous modelling study five feed distribution strategies were selected to be experimentally applied in order to check out the validity of the simulation. The same feeding parameters as the one used in the simulation (Table 1) were applied.

The main components of the experimental reactor are shown on Fig. 7. The overall setup was composed of a gas feeding system, a reactor with three injection ports and an online gaseous products analysis system. These three organs are described in the following sections.

3.1. Channel micro-reactor and distributor designs

The reactor was a stacked single channel microstructured reactor. Its main compounds were two engineered 316L stainless steel foils arranged between two housing devices.

The housing was equipped with inlets (gas distributor) and outlet connexions, as well as heating devices and K thermocouple. The temperature was adjusted with a PID controller. Inlet streams were regulated with Brooks mass flow regulators for H_2, CO and N_2.

The engineered foils were the channel plate and a catalytic plate. The channel dimensions were 800× 1 mm. It was mechanically engraved in a 250 μm thick 316L foil with a PROTOMAT

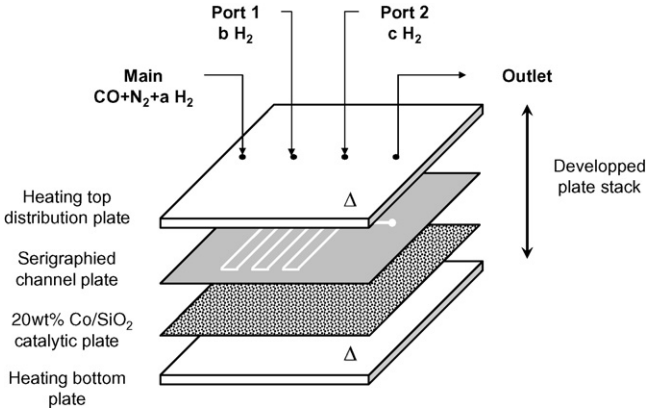

Fig. 7. Schematic view of un-stacked microchannel reactor ($a+b+c=1$).

fast prototyping machine controlled by Eagle software. The channel was stacked between the upper distributor and the lower catalytic plate.

The distributor was a three points 316L stainless steel injector. Syngas injected at main inlet leached the catalyst plate whereas auxiliary inlets were located orthogonally to the channel. All inlet gaseous streams are preheated at 180 °C. Their positions were calculated to be relevant of a developed linear distance of 267 and 533 mm from the channel main stream entrance; it divides the channel in three equal parts. Main inlet was an uncoated microchannel (30 mm × 1 mm × 0.25 mm) continuously prolonged by the reaction channel. Auxiliary inlet ports were 0.5 mm diameter pinholes. Outlet collector had characteristics similar to the main inlet.

Though convenient for rapid assembly and catalyst testing in microstructured environment, such a stacking solution applied to reactor structure limits the range of working pressure achievable. In absence of bonding of the structured foils, the maximum pressure achievable is very limited for metal/metal stacks: specifications for a similar commercially available catalyst testing microreactor are set at 0.3 MPa [38] whereas the design described here was tested as being leakage free up to 0.4 MPa [34]. It corresponds to the pressure gap usually reported for non-bonded stacked microstructures [39]. As a consequence it was decided to limit the working total pressure at 0.1 MPa.

3.2. Preparation of the catalyst

The preparation of the catalyst required a complex sequence, which has been documented elsewhere [34,40–42]. Main steps are summarized here.

The catalytic plate was made out of a multilayered composite material: AISI316L stainless steel substrate was pre-treated with remote plasma enhanced chemical vapour deposition (RPECVD); it allowed the growth of a 5 μm thick polymethylsiloxane film [40,41]. That film was then mineralized under the form of a SiO_x glass through a controlled thermal treatment under air. The obtained material acted as a bonding layer between the catalyst and the substrate [34,42]. That approach is similar to the one propose by Wang and co-workers [43], although it was specifically designed to be used with silica supported catalysts grafted of AISI316L steel in our case.

A 20 wt% Co/SiO_2 catalyst was used for the Fischer–Tropsch synthesis. It was obtained by a sol–gel modified method [42]. A classical sol made out of the catalyst and support precursors ($Co(NO_3)_2$ and $Si(C_2H_5O)_4$) acidified with HNO_3 was used. Contrary to the classic solution proposed elsewhere [37], a binary solvent (H_2O, C_2H_5OH) was used. Its composition was set at 42 wt% water for 58 wt% ethanol. Quantities of TEOS and $Co(NO_3)_2$ to be added were calculated to reach the desired catalyst final composition.

Coating was applied by a continuous hot spraying process. The 1 h aged sol was pulverized with an atomization nozzle on the RPECVD modified steel. Gelation occurred during aerosol phase transport and at the impact with the heated (150 °C) substrate. The fresh-coated catalysts were then treated under air at 350 °C for 1 h.

This method allowed getting catalysts layers with a thickness varying from 5 to 110 μm. Adhesion was A5 according to the ASTM-D3359-02 test. In this study a 5 μm bonding layer was used. It was coated with a 70 μm thick catalyst layer, which corresponded to 74.1 mg of 20 wt% Co/SiO_2 catalyst. Typical specific areas determined by nitrogen adsorption according to the B.E.T. method were set around 260 $m^2\,g^{-1}$. Pore volume was typically 0.17 $cm^3\,g^{-1}$ with 50% of microporous contribution [30]. XDR diffraction on picked up sample showed only Co_3O_4 oxide phase. All these properties were similar to the one obtained for similar catalysts used in a different microstructured reactor. Details on characterizations can be found elsewhere [42].

3.3. Evaluation of activity and product distribution

Catalyst was in situ conditioned under H_2 flow at 450 °C; a 5 °C min^{-1} ramp was used. Final temperature was hold for 4 h. The system was then cooled down to its working temperature. After thermal stabilisation, gaseous streams were swapped to the wished flow and composition values.

Outlet stream was heated at 250 °C to avoid product condensation. Gaseous products were analyzed on-line by gas chromatography using on one hand a DHES and a 13× molecular sieve columns in serial connected to a thermal conductivity detector and, on the other hand, a TDX-DB1 capillary column connected to a flame ionization detector. This set up allowed to get accurate information on CO conversion (X_{CO}) and product distribution (C_1–C_4, C_5–C_9, C_{10+}) within very short analysis times (1–15 min maximum for the complete gaseous products range); however the C_1–C_4 cut is represented by a single composite peak that cannot be deconvoluted and as such the C_1 (methane) selectivity could not be independently determined. Thus selectivities must be expressed as hydrocarbon cuts. Carbon mass balances were calculated on the basis of these analytical results. Ten mole percent of N_2 is injected simultaneously with CO; it is used as an internal standard for CO conversion calculation purpose. Measurements reported were done after 72 h under fixed reaction conditions.

3.4. Inlet feed conditions

The reactor was operated at $P = 0.1$ MPa and $T = 180$ °C. The feed strategy was defined in order to keep constant total molar flows of CO, N_2 and H_2 over the three inlets at 198, 66 and 396 mL h^{-1} STP, respectively. CO + N_2 were always injected at main inlet for all the reported experiments. All H_2 was injected at main inlet as a well-mixed gas with CO + N_2 for co-feed experiments; otherwise it was injected in various proportions given in Table 1 over the three possible H_2 injection ports, i.e. main, port 1 and port 2 (a–c respectively on Fig. 7).

The flow values selected for the modulation of the H_2 injection strategy correspond to an inlet partial pressure ratio of circa 2 for $P^0_{H_2}$ in respect of P^0_{CO} for co-feed experiments; this peculiar functioning point was selected for a comparison purpose as it corresponds to an almost optimum operation frame for FT with Co based catalysts under co-fed conditions [14].

4. Results

Table 3 gathers the various experimental performances in terms of CO conversion (X_{CO}) and product distribution (C_1–C_4, C_5–C_9, C_{10+} selectivities) obtained for the different staging strategies. Results are presented according to the experimental chronology. All the experiments were done on the same catalyst load. Co-feed experiments were done first and last in order to check out the catalyst stability over the entire experimental campaign.

4.1. Catalyst activity and product distribution in the Co-feed strategy

The activity achieved by the 70 μm thick 20 wt% Co/SiO_2 catalyst rose to a conversion level set around 18% (Table 3). This activity level was comparable with the ones previously observed for the same catalyst for a different micro-reactor flow configuration [42] or under a broader partial pressure and contact time experimental ranges [34]. Similarly product distribution exhibited a significant C_{10+} selectivity around 13% which was comparable with the observed performance for other Co/SiO_2 materials at 0.1 MPa and 180 °C [12].

C balance showed a slight deficit (Table 3): this is mainly due to its determination from the analysis of gas phase only that gives an incomplete overview of the formed products. It remained however quite satisfying because of the low expected production of C_{18+} products under the low pressure and temperature conditions applied. Activity and product distribution levels were fully recovered under similar feed conditions at fixed $T = 180$ °C and $P = 0.1$ MPa between the first co-feed experiment and the repeatability test at the end of the campaign (Table 3). Modification of the internal reactants partial pressures conditions through the H_2 distribution along the wall-coated catalyst did not seem to induce any significant deactivation of the active

Table 3
Experimental FT conversions and selectivities for co-feed, uniformly and non-uniformly staged H_2 feed over three equally spaced ports

	Strategy						
	Co-feed 1	≫	>	=	<	≪	Co-feed 2
X_{CO}	18.1%	16.1%	14.8%	13.8%	12.6%	12.0%	17.9%
C_1–C_4	64.3%	63.6%	62.8%	59.9%	54.5%	50.5%	65.7%
C_5–C_9	22.3%	23.7%	24.8%	27.9%	33.1%	33.2%	21.3%
C_{10+}	13.4%	12.7%	12.4%	12.2%	12.4%	16.3%	13.0%
C balance	94%	95%	93%	96%	94%	89%	92%

phase even if five different flow distributions were tested over a total 432 h under reaction. Thus the catalytic results obtained in between for distributed feed experiments were considered as being meaningful.

4.2. Catalyst activity and product distribution in the staged-feed strategy

The H_2 flows were distributed within a $CO + N_2$ continuous flow, shifting the local gas phase composition from H_2 rich feed ($\gg$) to H_2 depleted ($\ll$) conditions in respect of main inlet. The channel reactor was never set under totally H_2 depleted condition for main inlet, which always insured a minimum participation of the whole catalyst load over the entire length of the reactor. Complementary H_2 required for keeping a constant total H_2 molar flow over the summed three inlets was progressively shifted toward the two remaining auxiliary injectors. Thus it modulated the local P_{H_2}/P_{CO} partial pressure ensuring local compositions that were unable to be reached under co-feed situation for a fixed total reactant molar flow. This modulation was applied using a progression of the distribution tuning, from H_2 main inlet richer to poorer conditions. A central point consisted in a uniform distribution (=) of H_2 over the three possible injection ports.

It appeared that the activity level was progressively lowered, the later the H_2 being injected the lower CO conversion being (Table 3). The conversion levels were thus progressively lowered from 16.1 to 12% while the H_2 distribution profile was progressively shifted from main inlet rich to depleted conditions.

The product distribution was influenced by the feed geometry (Table 3). It appeared that delaying the injection of the main H_2 flow contribution over the last third of the reactor favoured a decrease of the C_1–C_4 selectivity. In the same time the C_5–C_9 selectivity rose from 23.7% for $\gg$ geometry (i.e. 66% of H_2 is injected in the main port) to 33% for the latest H_2 injection under $\ll$ geometry (where 66% of the H_2 is injected in head of the last reactor section). Singularly the C_{10+} selectivity showed little sensibility to the distribution policy, remaining somehow constant around 12%. The latest point at $C_{10+} = 16.3\%$ for $\ll$ injection geometry is relevant of a brutal increase of selectivity which may be questionable in respect of an odd C balance (89%). The obtained product distribution tending toward an increased formation of waxes, the latter will remain liquid and eventually held up within the structure which will cause a carbon mass balance deficit as only the composition of gaseous products at 180 °C is analyzed with the current analytical set-up.

5. Discussion

The proposed modelling must be carefully considered under the retained hypotheses. Pseudo-homogeneous modelling and gas phase composition evolution must therefore be addressed. The hypothesis of limited or negligible internal mass transfer limitation was found to be acceptable for layers thinner than circa 50–70 μm [42]. Thicker layers cannot be strictly considered as being consistent with the hypothesis of negligible intradiffusionnal limitations. But the apparent CO apparent consumption rate was computed from experimental results gathered over a 20–110 μm thickness range and therefore integrates any eventual internal transport limitations [34].

The hypothesis of a molar contraction factor being independent from the product distribution for any extend of reaction is the most arguable hypothesis. However in absence of a convenient model for FT selectivity over Co based catalysts at low pressure and temperature, an assumption had to be proposed to approximately model reactors with non-negligible internal composition gradients. Indeed the influence of molar contraction and the product partial pressure cannot be neglected anymore for integral X_{CO} levels, i.e. set above circa 4–8%, boundary remaining to be defined precisely. For high conversions with levels set up to 30% for the same 20 wt% Co/SiO_2 catalyst, the proposed hypothesis was previously found to be satisfying for the simulation of co-fed channel micro-reactors operated at low pressure and temperature [44]. Thus it can be here considered that such an identical hypothesis might be acceptable for simplified early pre-experimental simulation purpose.

The identification of $-r_{CO}$ to $-r_{CO+H_2}$ is in general a valid hypothesis only for a narrow P_{H_2}/P_{CO} gap centred around 2.1 for Co based catalysts [34,35]. Indeed the CO consumption rate used alone can rigorously be assimilated to the FTS apparent rate, $-r_{CO+H_2}$, only over a very narrow composition and temperature range [35]. At higher temperatures or H_2/CO ratio, $-r_{CO+H_2}$ is indeed influenced by the higher achieved H_2 consumption rate. In absence of coking and under negligible water gas shift (WGS) $-r_{H_2}/-r_{CO}$ tends toward a value of 3 under high T or P_{H_2}/P_{CO} because of an increased production of short hydrocarbons and water versus a value of 2 under milder conditions. The H_2/CO outlet ratio was reported as being non-constant from inlet to outlet for syngas feed ratio values set above 2.1–2.5 or temperature higher to 200 °C [34–35,44] thus indicating diverging CO over H_2 consumption rates and inducing a falsification of the estimated FTS apparent reaction rate from $-r_{CO}$ only. It appeared from previous study that this was acceptable on the 1.75–2.25 range for the 20 wt% Co/SiO_2 catalyst used here [34]. Beyond an inlet feed ratio set at 2.25, outlet composition was no longer assuring a value kept constant; to remain acceptable the staging strategy required keeping local partial pressure ratio below a top level of 2.25 which was the case here, the maximum attainable level at any point being imposed at 2. Below 1.75, activity levels reached at low temperature under 0.1 MPa are supposed to be too low to exhibit a detectable eventual over consumption of CO in respect of H_2. We concluded the simplification of $-r_{CO} = -r_{CO+H_2}$ was acceptable.

The experimental conversion obtained under staged feed policies were not very surprising: considering the known behaviour of the FT under a broad range of P_{H_2}/P_{CO} conditions under similar space hour velocity, temperature and total pressure, they followed the general trends reported for Co based catalysts. The conversion trend alone has been easily predicted by the pre-experimental modelling from a simple 1D model. Such a fairly simple modelling strategy may indeed be used for design and characterization of isothermal reactors as it was showed for an iron-based catalyst in [45]. Conversion variation trends were quite similar to the ones previously reported for various FT H_2

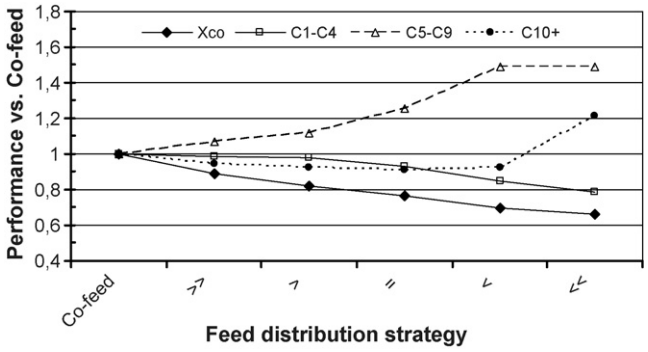

Fig. 8. Relative influence of staging policies over three equally spaced port on FT product distribution and activity.

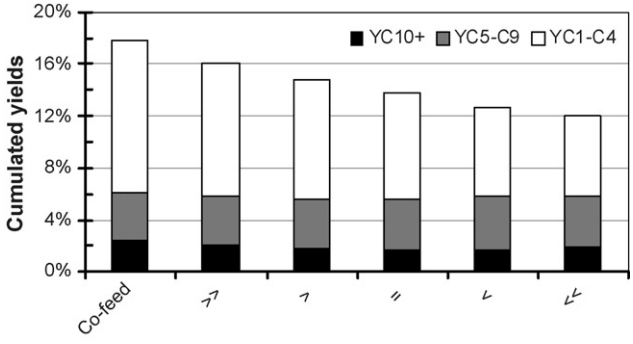

Fig. 9. Influence of staging policies over three equally spaced port on cumulated hydrocarbon yields.

distribution reactors whatever they were continuous distributors or discrete multipoint H_2 injectors [17–21]. However order of magnitude of experimental variations of X_{CO} slightly differed from values previously reported. Under low pressure and low temperature conditions for distribution membrane fixed-bed reactors Léonard reported a maximum of 60% of relative conversion decrease versus co-feed policy [18–21] whereas Sharifnia et al. [17] reached between 40 and 60% of loss for a discrete staged packed bed reactor. Here X_{CO} was in the range 12–16.1% which indicatively corresponded to 11–33.7% of conversion loss versus co-feed policy. It is slightly lower than previously reported variation amplitudes (Fig. 8). For packed membrane reactors, the conversion loss was not only attributed to depleted H_2 composition over a large volume of reactor but to a possible shortcutting of the catalytic packing too [21]; it may contribute to explain the difference between conversion variations found between [18] and the present work. In all cases, the activity decreases testify of over-dimensioning of substantial sections of the different catalytic reactors used for staged experiments; more advanced design issues are required in order to optimize the inner potential of every stage, for example through catalyst management such as suggested in [16].

Discussion on product distribution is more case sensitive as it should be undergone only for similar values of conversion. As such variation trends can only be roughly discussed. These variations trends for product distribution were quite comparable with previously reported results. The global aspects of product distribution obtained were compatible with the ones reported by Sharifnia et al. [17]: an increase of C_{5+} selectivity in respect of the spatial delaying of the H_2 injection was obtained. But it was however less influenced by the feed uniformity in [17]: it reached a stable value whatever the staging policy was whereas the variation is more sensitive to the distribution policy in our case (Fig. 8).

An insight of the hydrocarbon yields for the three cuts examined gives additional information as far as a comparison between co-feed and staged feed is concerned (Fig. 9). Reactor performance expressed as yields ($Y = X_{CO} \times$ relative selectivity) showed a relative steady level for both $Y_{C_5–C_9}$ and $Y_{C_{10+}}$ whereas only $Y_{C_1–C_4}$ was affected. The latter tended to be dramatically reduced from 11.6% under co-feed to 6.1% under the latest H_2 injection ($\ll$). This decrease was continuous and testified of a smarter H_2 use within the reactor, C_1–C_4 cut being undesirable.

The comparison of the simulation for X_{CO} with the experimental results appeared to be quite satisfying too: parity plot showed a dispersion of results within a ±15% acceptation window (Fig. 10). Similar confidence level was found for steady-state micro-channel reactor [44]. It may indicates a relative robustness of the model proposed even for the simulation of reactors having local P_{H_2}/P_{CO} values below the 1.5–3 frame initially used to fit the rate parameters. It therefore contributes to validate the pre-experimental modelling approach as a diagnostic mode for the early design of a staged FT reactor operated in the $P_{H_2}/P_{CO} = 1$–2 range.

Additionally the peculiar case of FT H_2 distributed reactors must be examined under the scope of syngas feedstock. The distribution of a significant part of total H_2 flow over the channel structure would mean for H_2 rich syngas a compulsory upstream H_2 separation in order to set the main inlet P_{H_2}/P_{CO} ratio at a selected level prior to FT. This additional unit operation could be arguable and as such the H_2 rich syngas obtained for example from natural gas would not necessary appear as an interesting issue. H_2 poorer syngas may however be a potential feedstock: they are generally worked up with iron-based catalysts that can

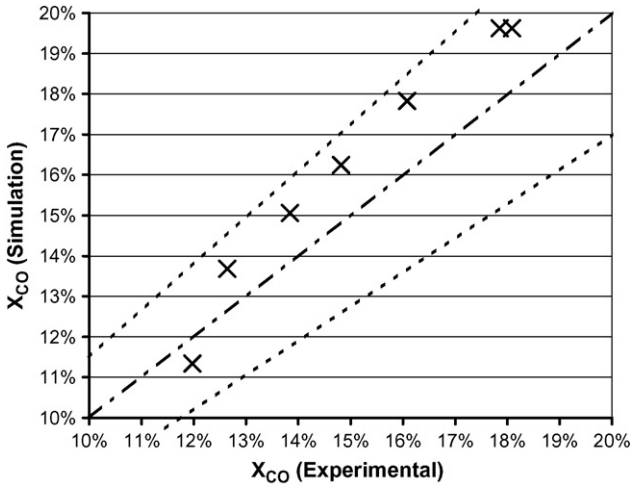

Fig. 10. Simulated X_{CO} vs. experimental X_{CO}; ±15% confident range indicatively shown.

deal with poor H_2 streams [10,14]. Cobalt catalysts with a longer life time and requiring lower temperature may replace the later providing an extra H_2 source may complete the required H_2 balance. Under such conditions the H_2 make-up could eventually be stage injected.

Concerning the reactor itself and its eventual scaling out, pragmatism would tend to favour the most cost competitive designs. It would either tend toward the selection of a limited number of additional inlets in regard of control capability or motivate a full swap toward continuous distributors that can be technically manufactured through membrane design. The tuning of number of inlets and their positions as well as the pattern of H_2 streams to be staged would require either extra study, specifically in term of product distribution modelling, or advanced material engineering, to propose a membrane able to deliver the targeted H_2 amount at the right place.

6. Conclusion

In the present contribution, the effect of H_2 staging for FT over a wall-coated catalyst in a channel microreactor was investigated. A pre-experimental modeling was used to predict the CO conversion levels attained for various discrete and continuous staging policies. Results were used to design a three port H_2 staged microreactor and to investigate the additional selectivity issues not covered within the model results. Obtained experimental results gave some insights of the effect of non-uniform staging for continuous distributors on X_{CO} which were comparable with the ones predicted by the simplified pre-experimental modeling protocol.

The experimental showed that beyond observed conversion modulation effect, the product distribution obtained though the tuning of H_2 flow pattern over a three ports distributor allowed an increase of the C_5–C_9 product selectivity. Once combined these conversion/selectivity effects allowed to half the $C_{1–4}$ yield without dramatically reducing the overall C_{5+} yield thus globally leading to a more efficient use of H_2. A non-uniform and increasing staging policy gave the best product distribution orientation for C_{5+} production at 0.1 MPa and 180 °C without jeopardizing the heavy product global yield traditionally achievable at this pressure.

Even if it only gave global yield trends under experimental conditions not suitable as such for industrial application, the use of a microstructured reactor added extra interest as it does not have to cope with scaling-up issues. It established a proof of principle and demonstrated the feasibility of a complex flow distribution configuration over the more classically reported single channel or parallel array fed with premixed syngas for a limited amount of discrete feed ports individually controlled.

Acknowledgments

This work benefited from access to the teaching and research facilities of the Ecole Centrale de Lille for reactor manufacturing. Dr. Guillou gratefully acknowledges the financial support of the Ministère de l'Education Nationale, de l'Enseignement Supérieur et de la Recherche.

Special acknowledgments are addressed to Mr. S. Thomy for mechanical engineering.

References

[1] Y. Lu, A.G. Dixon, W.R. Moser, Y. Hua Ma, Catal. Today 35 (1997) 443–450.
[2] Y. Lu, A.G. Dixon, W.R. Moser, Y. Hua Ma, Chem. Eng. Sci. 52 (1997) 1349–1363.
[3] Y. Lu, A.G. Dixon, W.R. Moser, Y. Hua Ma, Ind. Eng. Chem. Res. 36 (1997) 559–567.
[4] M. Sheintuch, O. Lev, S. Mendelbaum, B. David, Ind. Eng. Chem. Fundam. 25 (1986) 228–233.
[5] F.A. Al-Sherehy, A.M. Adris, M.A. Solimans, R. Hughes, Chem. Eng. Sci. 53 (1998) 3965–3976.
[6] T. Waku, M.D. Argyle, A.T. Bell, E. Iglesia, Ind. Eng. Chem. Res. 42 (2003) 5462–5466.
[7] V. Diakov, A. Varma, Ind. Eng. Chem. Res. 43 (2004) 309–314.
[8] F. Klose, T. Wolff, S. Thomas, A. Seidel-Morgenstern, Appl. Catal. A: Gen. 257 (2004) 193–199.
[9] A.P. Steynberg, M.E. Dry (Eds.), Fischer–Tropsch Technology, vol. 152, Elsevier, Amsterdam, Stud. Surf. Sci. Catal., 2004.
[10] R.B. Anderson, The Fischer–Tropsch Synthesis, Academic Press Inc., Orlando, 1984.
[11] T.-S. Zhao, J. Chang, Y. Yoneyama, N. Tsubaki, Ind. Eng. Chem. Res. 44 (2005) 769–775.
[12] S.T. Sie, M.M.G. Senden, H.M.H. Van Wechem, Catal. Today 8 (1991) 371–394.
[13] M.E. Dry, in: A.P. Steynberg, M.E. Dry (Eds.), Fischer–Tropsch Technology, vol. 152, Stud. Surf. Sci. Catal., 2004, pp. 533–600.
[14] G.P. van der Laan, Ph.D. Thesis, University of Groningen, Groningen, The Netherlands, 1999.
[15] M.E. Dry, A.P. Steynberg, in: A.P. Steynberg, M.E. Dry (Eds.), Fischer–Tropsch Technology, vol. 152, Stud. Surf. Sci. Catal., 2004, pp. 406–481.
[16] A. Tavasoli, A. Karimi, K. Zadeh, A. Khodadadi, Y. Mortazavi, S. Sharifnia, US20060079586 (2006).
[17] S. Sharifnia, Y. Mortazavi, A. Khodadadi, Fuel Process. Technol. 86 (2005) 1253–1264.
[18] S. Léonard S., Ph.D. Thesis, Université de Technologie de Compiègne, Compiègne, France, 2001.
[19] S. Léonard, S. Miachon, D. Vanhove, Récents Progr. Gén. Proc. 89 (2003) 226–234.
[20] D. Vanhove, S. Léonard, Récents Progr. Gén. Proc. 89 (2003) 297–304.
[21] L. Guillou, S. Léonard, V. Le Courtois, D. Vanhove, Proceedings of the Sixth International Conference on Catalysis in Membrane Reactors, Lahnstein, Germany, 2004.
[22] R.L. Espinoza, E. Du Toit, J.M. Santamaria, M.A. Menendez, J. Coronas, S. Irusta, Stud. Surf. Sci. Catal. A 130 (2000) 389–394.
[23] M.P. Rohde, D. Unruh, G. Schaub, Catal. Today 106 (2005) 143–148.
[24] A.L. Lapidus, A.Y. Krylova, A.N. Strupov, V.M. Linkov, R.D. Sanderson, Khi. Tver. Top. 28 (1994) 69–72.
[25] A.A. Khassin, T.M. Yurieva, A.G. Sipatrov, V.A. Krillov, G.K. Chermashentseva, V.N. Parmon, Catal. Today 105 (2005) 362–366.
[26] M.J.C. Bradford, M. Te, A. Pollack, Appl. Catal. A: Gen. 283 (2005) 39–46.
[27] V. Hessel, S. Hardt, H. Löwe, Chemical Micro-Process Engineering, vol. 1, Wiley, New York, 2004.
[28] X. Ouyang, R.S. Besser, Catal. Today 84 (2003) 33–41.
[29] Y. Wang, D.P. Vanderwiel, A.L.Y. Tonkovich, Y. Gao, E.G. Baker, USPTO 6 (491) (2000) 880.
[30] Y. Wang, J. Hu, R.T. Rozmiarek, J. Cao, A.L.Y. Tonkovich, T.J. Mazanec, Proceedings of the 13th International Congress on Catalysis, Paris, France, 2004.
[31] Y. Wang, C. Cao, X.S. Li, D.C. Elliot, USPTO 2005/0203195A1 (2005).
[32] www.velocys.com.
[33] K.T. Jarosch, A.L.Y. Tonkovich, S.T. Perry, D. Kuhlmann, Y. Wang, ACS Symp. 914 (2005) 258–272.

[34] L. Guillou, Ph.D. Thesis, Université de Technologie de Compiègne, Compiègne, France, 2005.
[35] I.C. Yates, C.N. Satterfield, Energy Fuels 5 (1991) 168–173.
[36] R. Zennaro, M. Tagliabue, C. Bartholomew, Catal. Today 58 (2000) 309–319.
[37] B. Ernst, Ph.D. Thesis, Université Louis Pasteur, Strasbourg, France, 1997.
[38] "Process Technology of Tomorrow", Part II, IMM catalogue, 2003.
[39] J.M. Commenge, First Thematic School on Reactor Engineering, Frejus, France, 2005, private communication.
[40] L. Guillou, Ph. Supiot, V. Le Courtois, Proceedings of the Seventh World Congress on Chemical Engineering, Glasgow, Scotland, 2005.
[41] L. Guillou, V. Le Courtois, Ph. Supiot, Mater. Tech. 93 (2005) 335–343.
[42] L. Guillou, D. Balloy, Ph. Supiot, V. Le Courtois, Appl. Catal. A: Gen. 324 (2007) 42–51.
[43] Y.-H. Chin, J. Hu, C. Cao, Y. Gao, Y. Wang, Catal. Today 110 (2005) 47–52.
[44] L. Guillou, V. Le Courtois, GeCat, Mittlewhir, France, 2006.
[45] J.C.A. Green, B. Jager, Chem. Eng. Sci. 40 (1985) 635–640.